International Journal of Psychophysiology 120 (2017) 136–147

Contents lists available at ScienceDirect

International Journal of Psychophysiology

journal homepage: www.elsevier.com/locate/ijpsycho

# Impedance cardiography in healthy children and children with congenital heart disease: Improving stroke volume assessment

Ineke Nederend[a,b,*], Arend D.J. ten Harkel[b], Nico A. Blom[b], Gary G. Berntson[c], Eco J.C. de Geus[a]

[a] Vrije Universiteit Amsterdam, Amsterdam Public Health Research Institute, Department of Biological Psychology, Faculty of Behavioral and Movement Sciences, Van der Boechorststraat 1, 1081 BT Amsterdam, The Netherlands
[b] Department of Pediatric Cardiology, LUMC University Medical Center, Albinusdreef 2, 2333 ZA Leiden, The Netherlands
[c] Ohio State University, Department of Psychology, 1835 Neil Avenue, Columbus OH 43210, United States

ARTICLE INFO

*Keywords:*
Impedance cardiography
Stroke volume
Children
Congenital heart disease
Pre-ejection period
Left ventricular ejection time

ABSTRACT

*Introduction:* Stroke volume (SV) and cardiac output are important measures in the clinical evaluation of cardiac patients and are also frequently used in research applications. This study was aimed to improve SV scoring derived from spot-electrode based impedance cardiography (ICG) in a pediatric population of healthy volunteers and patients with a corrected congenital heart defect.

*Methods:* 128 healthy volunteers and 66 patients participated. First, scoring methods for ambiguous ICG signals were optimized to improve agreement of B- and X-points with aortic valve opening/closure in simultaneously recorded transthoracic echocardiography (TTE). Building on the improved scoring of B- and X-points, the Kubicek equation for SV estimation was optimized by testing the agreement with the simultaneously recorded SV by TTE. Both steps were initially done in a subset of the sample of healthy children and then validated in the remaining subset of healthy children and in a sample of patients.

*Results:* SV assessment by ICG in healthy children strongly improved (intra class correlation increased from 0.26 to 0.72) after replacing baseline thorax impedance ($Z_0$) in the Kubicek equation by an equation ($7.337–6.208 * dZ/dt_{max}$), where $dZ/dt_{max}$ is the amplitude of the ICG signal at the C-point. Reliable SV assessment remained more difficult in patients compared to healthy controls.

*Conclusions:* After proper adjustment of the Kubicek equation, SV assessed by the use of spot-electrode based ICG is comparable to that obtained from TTE. This approach is highly feasible in a pediatric population and can be used in an ambulatory setting.

## 1. Introduction

Congenital heart defects (ConHD) affect around 9 per 1000 newborns (van der Linde et al., 2011) and is the most common congenital defect. Due to modern surgical techniques, survival in childhood is good (Moons et al., 2010), but complications in adulthood, including pulmonary hypertension (Engelfriet et al., 2007; van Riel et al., 2014) and arrhythmias (Bouchardy et al., 2009; Walsh and Cecchin, 2007), are not uncommon. Many patients eventually die from heart failure, sudden cardiac death or other cardiac problems (Zomer et al., 2012; Verheugt et al., 2010). However, the exact mechanisms through which these late problems develop is not yet fully understood, and the individual characteristics that could predict who is most at risk remain to be identified.

Stroke volume (SV) and the product of SV and heart rate (cardiac output; CO) are important measures in the clinical evaluation of cardiac patients (Warnes et al., 2008) and are also frequently employed for research purposes. However, most of the methods used to measure SV are moderate to highly invasive which make them unsuitable for use in young patients and restricts their use to clinical settings.

Much effort has been put into measuring SV and CO in a non-invasive way (Marik, 2013; Critchley and Critchley, 1999) with impedance cardiography (ICG) emerging as the most promising method (Raaijmakers et al., 1999; Cybulski et al., 2004; Kubicek et al., 1966). The burden imposed by ICG is sufficiently low for it to be used even in very young children (van Dijk et al., 2013; Morgan et al., 2011). As an additional advantage it can be employed in naturalistic settings for up to 24 h, without the need for continuous supervision by a clinician

* Corresponding author at: Vrije Universiteit Amsterdam, Amsterdam Public Health Research Institute, Department of Biological Psychology, Faculty of Behavioral and Movement Sciences, Van der Boechorststraat 1, 1081 BT Amsterdam, The Netherlands.
*E-mail addresses:* i.nederend@vu.nl (I. Nederend), A.D.J.ten_Harkel@lumc.nl (A.D.J. ten Harkel), N.A.Blom@lumc.nl (N.A. Blom), berntson.2@osu.edu (G.G. Berntson), eco.de.geus@vu.nl (E.J.C. de Geus).

http://dx.doi.org/10.1016/j.ijpsycho.2017.07.015
Received 12 January 2017; Received in revised form 20 July 2017; Accepted 29 July 2017
Available online 01 August 2017

(Neijts et al., 2015; Goedhart et al., 2007; Vrijkotte et al., 2004). For an ICG, no behavioral demands have to be made on the patient whereas Magnetic Resonance Imaging and transthoracic echocardiography require one to lay still and sometimes perform breath holds which can be problematic in young children.

The development of ICG technology was originally sponsored by NASA specifically to measure SV and derived hemodynamics during manned flight (Kubicek et al., 1966). Although the original method employed circumferential band electrodes, alternative spot electrode configurations have more recently been introduced (Boomsma et al., 1989; Penney et al., 1985; Qu et al., 1986). Various studies comparing ICG-derived SV to alternative SV scoring modalities in standardized clinical settings have found good criterion validity (Lorne et al., 2014; Schmidt et al., 2005; Summers et al., 2003; Critchley and Critchley, 1999; Shoemaker et al., 1998; Ebrahim et al., 2016) even during exercise (Richard et al., 2001; Kemps et al., 2008; Charloux et al., 2000), although not all studies find good agreement (Fellahi et al., 2009; Doering et al., 1995; Kamath et al., 2009; Engoren and Barbee, 2005). In 1992 and 1999, meta-analyses were carried out on studies testing the agreement between ICG derived SV and from reference modalities showed an overall correlation coefficient of 0.81 and 0.82 (Raaijmakers et al., 1999; Fuller, 1992). A more recent meta-analysis comparing ICG to thermodilution reported a correlation coefficient of 0.79 (Peyton and Chong, 2010). Validation studies on pediatric cardiac patients (Norozi et al., 2008; Grollmuss et al., 2012), pediatric intensive care patients (Blohm et al., 2014), obese children (Brown et al., 2005; Rauch et al., 2013) and healthy neonates (Noori et al., 2012) show good agreement. However, Taylor et al. and Schubert et al. concluded that ICG did not perform properly in estimating SV in children during nor directly after surgery for their ConHD (Schubert et al., 2008; Taylor et al., 2011; Taylor et al., 2012). ICG proved to be more challenging in ambulatory settings (Cybulski et al., 2004; Willemsen et al., 1996; Riese et al., 2003) where temporal stability of ambulatory ICG derived SV was moderate at best, compared to excellent temporal stability found for ICG-derived systolic time intervals, even during resting periods that excluded potential movement artefacts (Goedhart et al., 2006). This suggests that the approach to score the SV from a spot electrode-derived ICG is not yet optimal.

In the impedance cardiogram, which is the first derivative of the thoracic impedance (Z) with respect to time (dZ/dt), three points can be derived: 1. The 'B-point' that represents the moment of opening of the aortic valve, reflected in a notch in the ICG signal. 2. The 'C-point' corresponding to the peak blood flow in the aorta, reflected in a minimum in the ICG signal. 3. The 'X-point' that corresponds to the moment of closing of the aortic valve, reflected in an incisura in the idealized ICG signal (Fig. 1, *top panel*). By combining the ICG and the electrocardiogram (ECG), it is possible to derive the pre-ejection period (PEP) as the time between the start of ventricular depolarization (Q onset in the ECG) and the opening of the aortic valve (B-point in the ICG). A second systolic time interval, the left ventricular ejection time (LVET), is derived as the difference between the B- and X-points in the ICG. The LVET can be used in conjunction with the amplitude of the C-point to compute SV using the Kubicek equation (Kubicek et al., 1966):

$$SV = \rho\,(L/Z_0)^2 \bullet LVET \bullet dZ/dt_{max} \quad (1)$$

where SV is the stroke volume (mL); ρ = blood resistivity (fixed at 135 Ω ∗ cm); L = measured length between the measuring electrodes (cm); $Z_0$ = baseline thorax impedance (Ω); LVET = left ventricular ejection time (s); $dZ/dt_{max}$ (Ω/s) = the amplitude (i.e. absolute value), measured from either the dZ/dt = 0 baseline or the dZ/dt amplitude registered at the B-point (Sherwood et al., 1990). Note that thorax impedance decreases during the systolic phase, but in keeping with typical visual depiction of cardiac signals, the ICG signal is usually drawn in reverse polarity and the dZ/dt minimum is shown as a dZ/dt maximum. This convention will be retained throughout this report and the dZ/dt minimum will be referred to as $dZ/dt_{max}$.

Various groups that have intensively used the ICG in psychophysiological research, including our own, have noted that instead of an idealized ICG wave form (Fig. 1, *top panel*) many subjects present with a more complex ICG wave form (Fig. 1, *lower panel*) introducing ambiguity in the scoring of the B-point, as well as that of the C– and X-points (van Lien et al., 2013; Lozano et al., 2007; Sherwood et al., 1990; Kelsey and Guethlein, 1990). Typically, the ambiguity in B-point scoring is caused by a double notch. B-point ambiguity is most clearly seen in cardiac patients, especially at older ages (Ermishkin et al., 2014). Ermishkin and colleagues hypothesize that the B-point is the intersection of two waves: the pre-ejection wave (caused by changes in heart geometry and that of surrounding vessels due to cardiac contraction in the isovolumetric phase) and the ejection wave (caused by increased volume in the aorta and surrounding vessels). Timing of the pre-ejection wave could explain the double notch in the ICG signal. The double C-point may be attributable to different aortic flow patterns (van Eijnatten et al., 2014), in healthy subjects during exercise but in cardiac patients may also be present in rest. The presence of multiple of these ICG landmark candidates can also be caused by the non-synchronous contraction of the ventricles, for example because of conduction disorders such as a bundle branch block, sometimes seen in patients with prior operations on the intra-cardiac septum. Typically, the uncertainty in scoring of the X-point is attributable to a W-shaped (double U) waveform, where the trough in either the first or second 'U' may be the point corresponding to the closure of the aortic valve. The W-shape likely represents the successive closing of the aortic and the pulmonic valve (Miles and Gotshall, 1989; Lababidi et al., 1970) which in healthy subjects can occur during inspiration but can also be caused by an atrial septal defect or a bundle branch block. Exercising at increasing levels of intensity further modulates the shape of the ICG at the X-point (Ono et al., 2004).

The ambiguities in B- and X-points are further aggravated by respiration, postural and movement artefacts, and in our experience occur more often in ambulatory recordings than in recordings from laboratory settings. ICG signal quality can be improved by band pass filtering and ensemble averaging, but no amount of signal conditioning completely dispenses with the ambiguity of the critical landmarks in the ICG. Ambiguity in the B-point immediately affects the validity of the PEP and LVET, but it also distorts the $dZ/dt_{max}$ amplitude that is used in SV estimation. Ambiguity in the X-point and C-point further distorts SV estimation by influencing the left ventricular ejection time (LVET) and $dZ/dt_{max}$ amplitude respectively. Empirical validation of B- and X-point scoring in the ICG against a criterion measure of aortic valve opening and closure is direly needed.

To obtain the ICG signal, current electrodes on the back send a small alternating current through the thorax and measuring electrodes on the chest detect changes in thoracic impedance related to the aortic blood flow. In the original development of the technique band electrodes around the neck and waist were used, but soon spot electrodes on the back and chest were found to yield ICG signals of comparable quality (Qu et al., 1986; Penney et al., 1985; Boomsma et al., 1989; Sherwood et al., 1992). Compared to band electrodes, spot electrodes greatly decrease obtrusiveness and measurement burden on the subjects, increasing feasibility of longer recordings and improving ecological validity (Houtveen et al., 2006). However, there are two important distinctions in the ICGs generated from spot and band electrodes. The baseline impedance of the thorax is much higher using band electrodes and L parameter (distance between the measuring electrodes) is often larger since the band electrodes have to be attached further apart than the spot electrodes in most spot electrode configurations (Boomsma et al., 1989; Sherwood et al., 1992). This has repercussions for the Kubicek equation where SV is estimated using the product of the dZ/dt amplitude and the LVET, weighing for blood resistivity, the distance between the measuring electrodes, and the baseline thorax impedance. Typically, absolute SV seems to be overestimated if no correction of the Kubicek equation is made to account for the use of spot electrodes

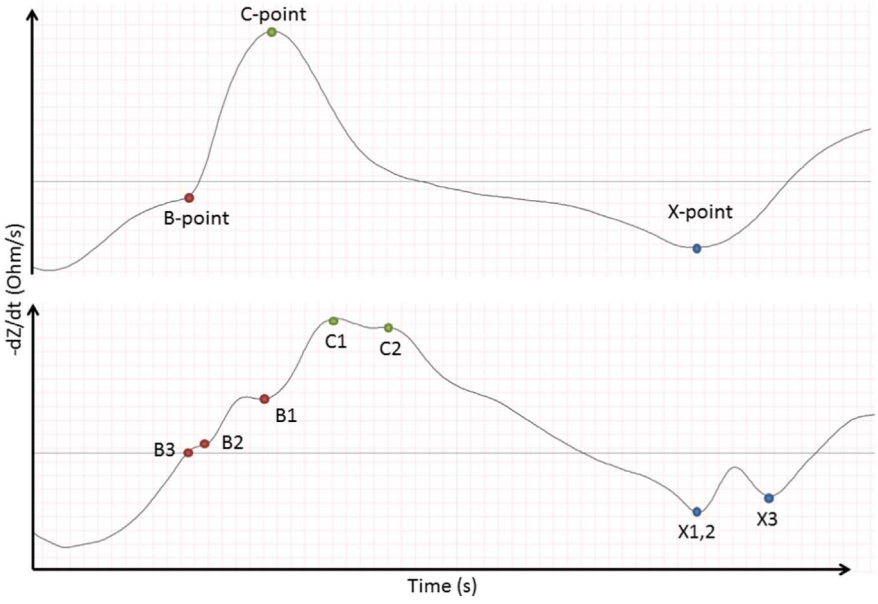


**Fig. 1.** Top panel: unambiguous ICG including B– C– and X–point. Lower panel: complex ICG waveform with multiple cadidates for B– C– and X–points.

(Boomsma et al., 1989).

The main aim of this study was to improve SV assessment from a spot-electrode based ICG in a pediatric population of both healthy children and children with a corrected ConHD. We used a two-step approach that we present in two separate analyses based on the same experiment. Both sets of analyses consist of a discovery and a replication phase and employ the same group of healthy controls and patients. We present these analyses as study 1 (optimization of scoring methods for ambiguous ICG landmarks) and study 2 (tailoring the Kubicek SV equation to spot electrodes). An overview of the complete design is depicted in Fig. 2. In study 1, optimal methods to select the correct point from multiple potential B-, C– and X-points in the ICG signals were determined in a discovery set of healthy children by comparing the ICG-derived systolic time intervals to those derived from simultaneously recorded Doppler signal by transthoracic echocardiography (TTE). Ambiguity for the C-point is usually caused by the presence of a bimodal peak, where it is still unclear if the first or the second of such C-points corresponds to the fastest acceleration of aortic blood flow. As acceleration can be detected visually with reasonable fidelity in the echocardiogram of most subjects, our data will allow us to resolve this by visual inspection. Ambiguity in the B-point and X-point in the ICG can be resolved by TTE as they should coincide with the moments of opening and closure of the aortic valve which can be detected accurately in the echocardiogram. The method for the B- and X-point selection that yield the highest Intra Class Correlation (ICC) compared to echocardiography was taken forward in two replication datasets: a second group of healthy children and a group of patients with a corrected ConHD (ventricular septal defect and coarctation of the aorta). ICCs for TTE- and ICG-derived PEP and LVET in these datasets will be used to test the criterion validity of the new B- and X-point selection method.

In study 2, using the optimal scoring methods for B-, C- and X-points from study 1, SV scoring was optimized by adjusting the Kubicek equation for the value of the baseline impedance ($Z_0$) in the spot electrode configuration. Based on the difference in the SV as measured by the ICG and the echocardiogram, a corrected $Z_0$ was computed in the discovery set that maximizes the ICC between SV derived from echocardiography and SV derived from ICG for each individual subject, additionally taking into account that subject's value for L, $dZ/dt_{max}$, age, sex, height and weight. The resulting $Z_0$ correction approach was applied to the two independent replication sets (healthy controls and children operated for their ConHD). ICCs for SV were used to test the criterion validity of this new ICG-based SV-scoring approach in both healthy children and children with ConHD, again by comparing to echocardiography. Because SV can be derived from the echocardiogram through different methods, we repeated the SV validation using the three most often used methods; biplane, velocity time integral and 3D.

## 2. Participants and procedure

### 2.1. Participants

Healthy controls between 1 and 18 years of age were recruited to take part in the studies. Children from 1 to 4 years were recruited from the outpatient department of pediatric cardiology. Those who had an innocent murmur or other complaints that turned out to be unrelated to a cardiac disorder were asked to participate. Healthy controls aged 4–18 were passively recruited through an advertisement at school. Chronic disease or medication use was exclusion criteria. When the echocardiogram showed a structurally and functionally normal heart, the volunteer was included in the study. Patients with repaired ConHD from the outpatient clinic aged 8–18 years old were asked to participate. Patients after isolated ventricle septum defect (VSD) repair and patients after isolated coarctation (CoA) repair were included in the study. Children with chromosomal disorders were excluded. All participants and both (one in the case of single-parent families) of their parents/guardians provided written informed consent. All study procedures were reviewed and approved by the medical ethics review committee of the LUMC medical centre (P13.198 and P14.095)

The 128 healthy control subjects were randomly divided into a discovery set ($N = 88$) and a replication set (replication set 1, $N = 40$). The group of ConHD patients were allocated to replication set 2 ($N = 66$).

### 2.2. Procedure

Data collection took place at the LUMC medical centre. First, the procedure was explained to the participants and their parents. Next, participants were weighted and length was measured. Then, electrodes for thoracic impedance monitoring were attached, connected to the device and the participant was laid down for the echocardiogram with simultaneous measurement of the ICG which took on average 20 min.

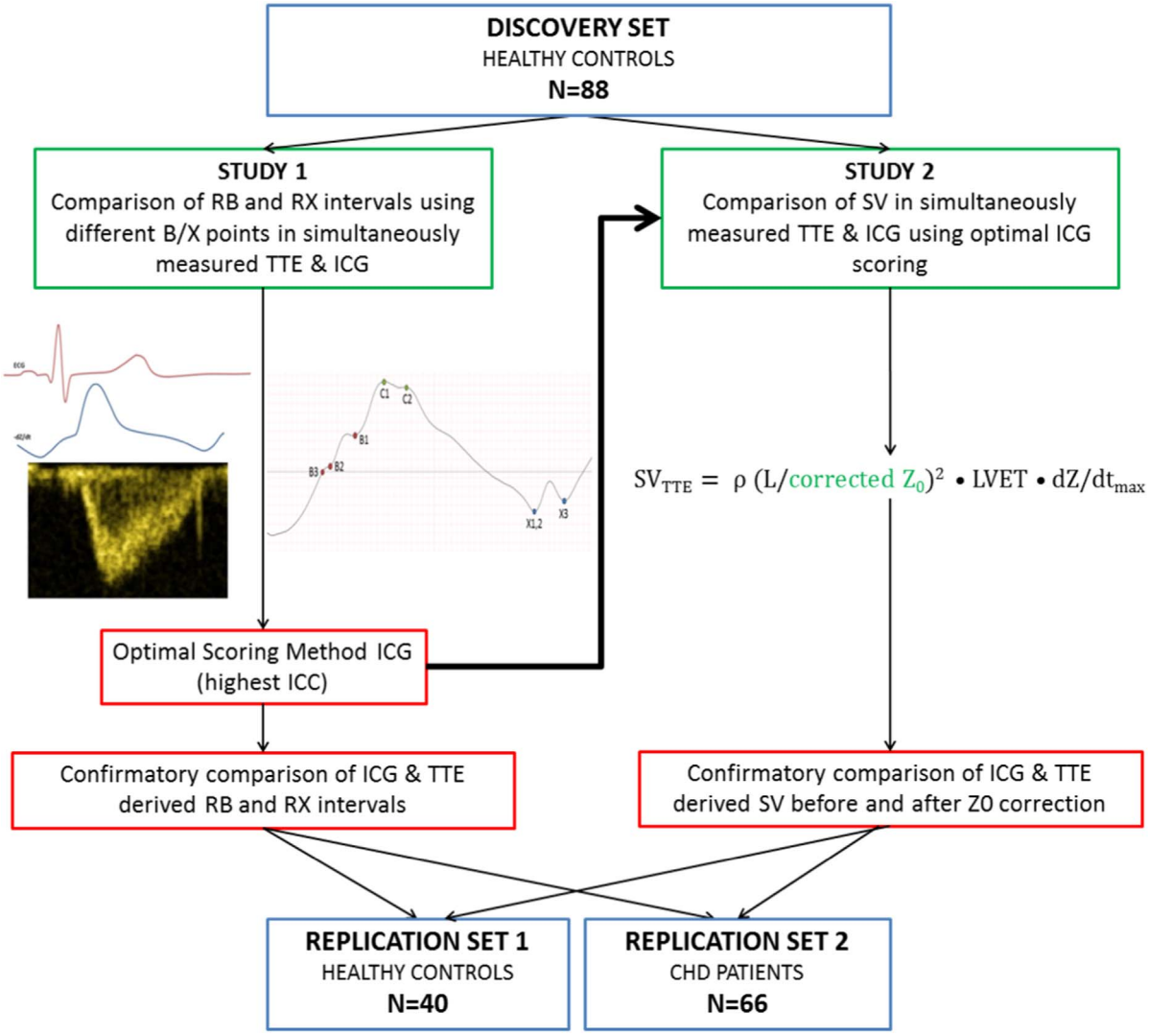


**Fig. 2.** Study design.

### 2.3. Electrocardiogram registration and thoracic impedance

ECG and ICG registration was done using the 5 fs version of the VU Ambulatory Monitoring System (VU-AMS; VU University, Amsterdam, The Netherlands, www.vu-ams.nl) (de Geus et al., 1995). One lead ECG was derived from 3 pregelled Ag/AgCl (Kendal H124SG) spot electrodes on the chest. ECG was sampled at 1 kHz and R peaks are automatically detected by the device. We measured thoracic impedance (Z) against a small alternating current (50 kHz, 350 μA) induced by two spot electrodes at the back. Thoracic impedance was recorded with a sample frequency of at 250 Hz. The measuring electrodes were placed just above and below the sternum. Current electrodes were placed 3 cm above and below the measuring electrodes (placement depicted in Fig. 3) on the back of the thorax. A fixed period of 1 min synchronous to the echocardiography acquisition was selected from the VU-AMS data. Ectopic beats were removed from the data. Ensemble averaged ICG and ECG over that period were used for analysis.

### 2.4. Transthoracic echocardiogram

Transthoracic echocardiograms (TTE) were conducted by a pediatric cardiologist or an experienced technician (Vivid 9, GE healthcare, Norway) and evaluated by one researcher, supervised by a pediatric cardiologist. EchoPac version 113 was used for analysis of the images.

## 3. Study 1 (optimization of scoring methods for ambiguous ICG landmarks)

### 3.1. Methods

#### 3.1.1. Echocardiogram

Systolic time intervals were assessed using a pulsed wave Doppler flow signal just after the aortic valve in a parasternal 5 chamber view. Time between the R peak and the opening and closing of the aortic valve were measured (Fig. 4). This was repeated in three different heart beats for every subject, the average of those three measurements was used for analysis

#### 3.1.2. Optimizing B-point selection

Based on the literature and our previous experience, 3 candidates (Fig. 1, *lower panel*) were considered to potentially reflect the true B-point during interactive visual scoring. The candidate B-point had to occur in a 150 msec window after the R-peak.

Candidate B-points:

1. Candidate before highest upstroke of dZ/dt (B1)
2. Candidate closest to dZ/dt = 0 (B2)
3. dZ/dt = 0 (B3)

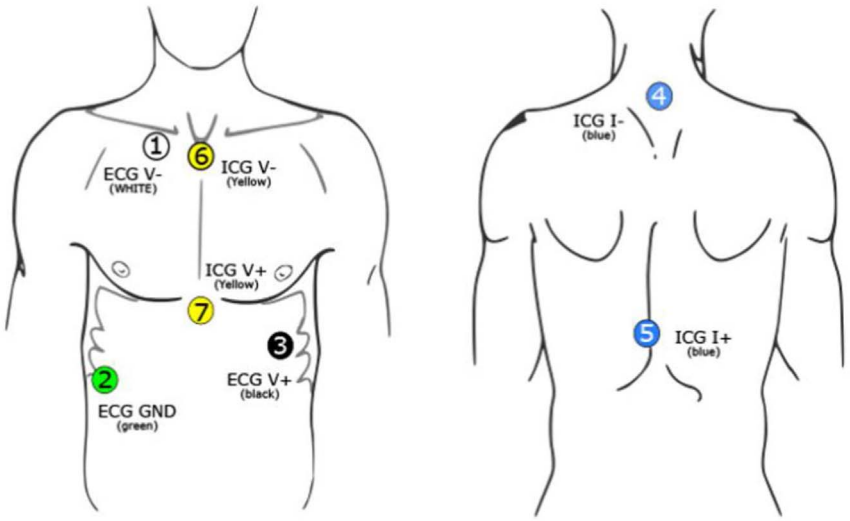


**Fig. 3.** Placement of the seven spot electrodes.

For each of these candidate B-points the interval (ms) between the R-peak and the B-point was calculated. If only candidate B-point 1 was discernible, no ambiguity was present and the intervals for the B-point for candidate 2 were set to an identical value as the interval for candidate B-point 1. Fig. 5 shows an example with 3 different intervals (red lines). We then compared the RB intervals for each of the three candidates to the criterion RB intervals extracted from the echocardiogram. For the extraction of these RB intervals we visually marked the moment of opening of the aortic valve from the Doppler signal (Fig. 4). We did this comparison across all subjects and separately for illustrative purposes using only subjects with an ambiguous B-point. The scoring method (B1, B2 or B3) with the highest ICC (across all subjects) between the intervals in the discovery set was subsequently applied in the replication sets.

### 3.1.3. Optimizing C-point selection

The echocardiogram was visually inspected for the moment of maximal blood flow acceleration in the ascending aorta. The maximal acceleration is located at the steepest tangent to the Doppler flow signal.

### 3.1.4. Optimizing X-point selection

Based on the literature and our previous experience, 3 candidates (Fig. 1, *lower panel*) were considered to potentially reflect the true X-point during interactive visual scoring.

Candidate X-points:

1. Lowest point in dZ/dt signal (X1)
2. First trough (X2)
3. Second trough (X3)

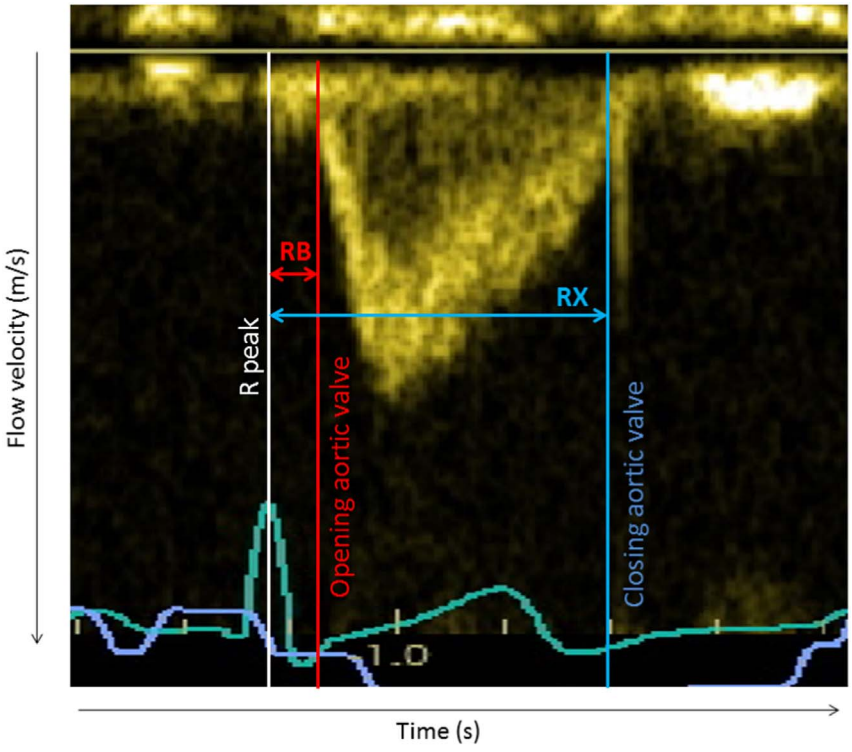


**Fig. 4.** Time intervals measured by TTE. RB: time between R peak and opening of the aortic valve; RX: time between R peak and closing of the aortic valve.

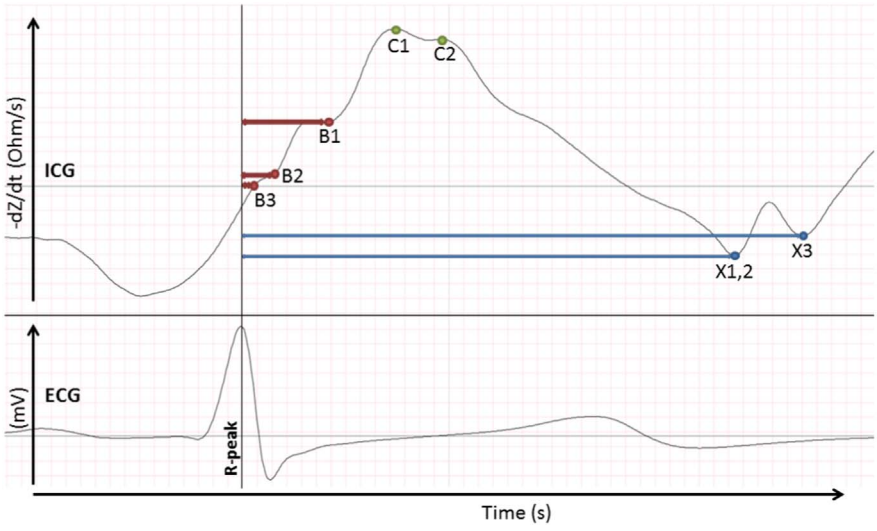


**Fig. 5.** Time intervals measured in the ICG. RB intervals for the different potential B points (red lines) and RX intervals for the different potential X points (blue lines). (For interpretation of the references to colour in this figure legend, the reader is referred to the web version of this article.)

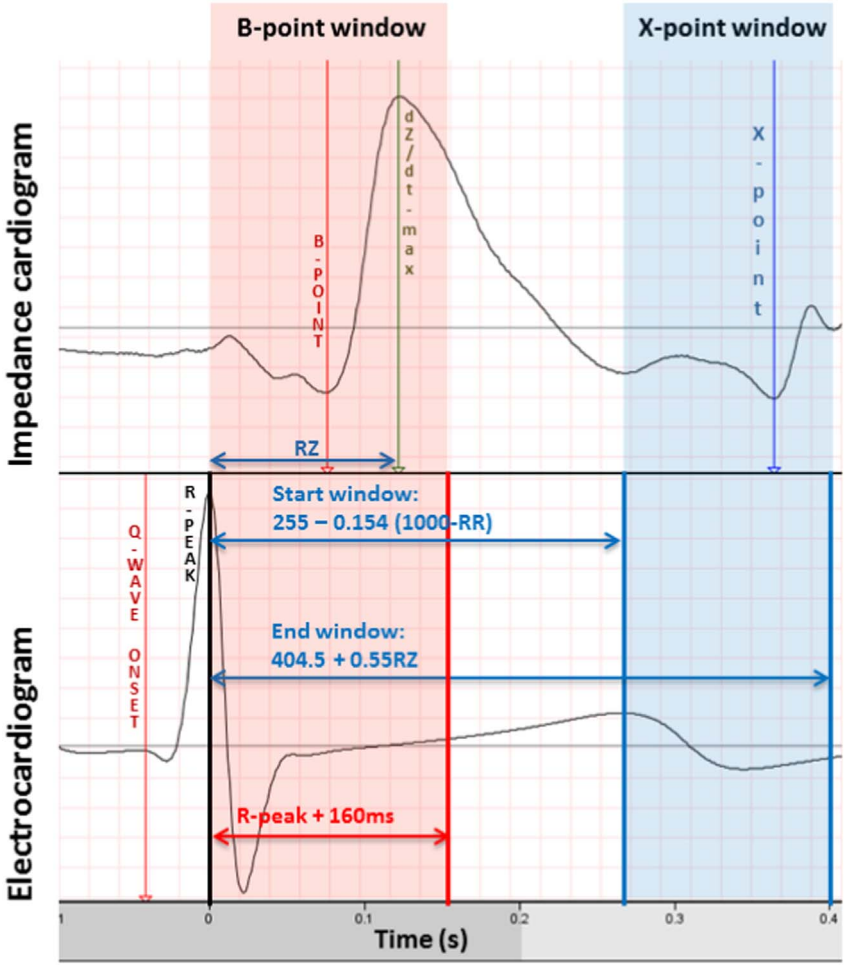


**Fig. 6.** Physiologically plausible windows for the B-point and X-point. HR = heart rate; ms = milliseconds; RR = inter-beat interval.

In the example in Fig. 1, X1 and X2 coincide. It is also possible that X1 and X3 coincide.

For each of these candidate X-points the interval (ms) between the R-peak and the X-point was calculated in the ICG, again in the discovery set ($N$ = 88). If only candidate X-point 1 was discernible, no ambiguity was present and the RX intervals for candidates 1, 2 and 3 were set to an identical value. Fig. 5 shows an example with 2 different intervals (blue lines); intervals for X1 and X2 are equal as this point is the lowest point in the signal and the first trough. We then compared the RX intervals for each of the three candidates to the criterion RX intervals extracted from the echocardiogram. For the extraction of these RX intervals we visually selected the moment of closing of the aortic valve from the Doppler signal (Fig. 4). We did this comparison across all subjects and separately for illustrative purposes using only subjects with an ambiguous X-point. The scoring method (X1, X2 or X3) with the highest ICC (across all subjects) between the intervals in the discovery set was subsequently

applied in the replication sets.

As an additional check we created a physiologically plausible window around the T-wave in which the X point should fall. For each X-point candidate (X1, X2 and X3), it was checked whether they fell in this window. Because ventricular repolarization must occur before the ventricular pressure decreases sufficiently to allow the aortic valve to close, we expect the X point to always fall after the peak of the T wave. The QT interval duration is dependent on heart rate; QT-interval time corrected for prevailing heart rate can be described as $QT_{corrected} = QT + 0.154(1000\text{-}RR)$ where RR is the inter-beat-interval in ms (Sagie et al., 1992). Also, the general consensus is that the shortest QT is 360 ms in healthy persons (Viskin, 2009), thus making the equation for the shortest QT interval expected 360–0.154(1000-RR). Since detecting an R-peak is much easier than detecting the Q-onset we subtract a QR interval of 55 ms in order to measure from the R-peak. Additionally, since the QT interval is measured to the end of the T-wave -which is roughly 100 ms- and we want to set the window from the T-wave peak, we subtract an additional 50 ms. Thus, the expected heart rate corrected $RT_{wave}$ interval –and thus the start of our physiologically plausible X-point window– would be $(360 - (55 + 50) - 0.154(1000 * RR) = 255 - 0.154(1000\text{-}RR)$. The end of the X-point window was defined by the use of the longest expected LVET based on a large published data set (van Lien et al., 2014); LVET during sleep was 314.9 ± 28.1 in this study of 564 healthy individuals. The mean LVET plus 3 standard deviations (= 400 ms) was taken as the longest expected LVET. Again, in order to measure from the easily detected R-peak, the RB interval must be added which was studied by Lozano et al. who found RB = 0.55RZ + 4.5 where RZ is the time interval from R-peak to C point (Lozano et al., 2007). Summing the RB interval and the longest expected LVET, the end of our X-window is described as: 404.5 + 0.55RZ. In Fig. 6, the physiological plausible X-point window is visualized.

### 3.1.5. Statistical analyses

IBM SPSS statistics software (version 23.0, Armonk, NY) was used for statistical analysis. The random number generator was used to allocate healthy control subjects to the discovery or replication set. For the comparison of the different B and X points and SV, intra class correlation (ICC; two way mixed, consistency agreement, single measures) was calculated.

## 3.2. Results

### 3.2.1. General descriptives

General descriptives of the healthy control group and the patient group can be found in Table 1. Age, gender, length and weight were not different in the discovery set and replication set of healthy controls. Patients, however, were slightly older and therefore longer and heavier

### 3.2.2. B-, C- and X-point scoring

Table 2 shows the number of cases in which we found 1, 2 or 3 candidate points. In six children no reliable B- or X-point could be detected. A majority of the children showed multiple candidates for the B- (57%) and X-points (69%) whereas for the C peak often only a single candidate was present (70%). Best agreement with echocardiography for the B-point across all subjects was found for candidate B1: the point just before the longest uninterrupted upstroke of dZ/dt (Table 3; ICC = 0.48 95%CI:0.27;0.65). The B1 point also performed best in the subset of subjects with ambiguous B-points. When applying this B1 scoring method to the replication set of healthy controls, agreement for the RB interval was 0.50 (Table 4; 95%CI:0.22;0.70). In the ConHD patients, ICC for the RB-interval with this B-point was 0.48 (Table 4; 95%CI:0.25;0.66).

In those instances where multiple C-points were present, visual inspection of the echocardiogram systematically favoured the peak nearest to the B-point (C1) as being closest to the point of maximal blood flow acceleration. This suggests that the moment of maximal blood flow acceleration in the aorta comes very soon after the opening

**Table 1**
General descriptives of the healthy controls (discovery and replication set 1) and of the ConHD patients (replication set 2).

| | Healthy controls discovery | Healthy controls (Replication set 1) | ConHD patients (Replication set 2) |
|---|---|---|---|
| N | 88 | 40 | VSD: *N* = 34<br>CoA: *N* = 32 |
| Male (%) | 56 | 45 | 43 |
| Age (y) | 9.1; 9.3 | 11.0; 8.2 | 12.3; 5.3 |
| Length (cm) | 140.0; 55 | 151.5; 43.8 | 156.0; 23.7 |
| Weight (kg) | 32.5; 34.1 | 39.1; 30.7 | 45.5; 24.8 |

Note. Median; IQR. ConHD: congenital heart disease. VSD: ventricle septal defect. CoA: coarctation of the aorta.

**Table 2**
Number of candidate B- and X-points in the discovery set.

| | *N* | % |
|---|---|---|
| Missing | 6 | 7 |
| Single B-point (B1 = B2) | 32 | 39 |
| Double B-point (B1 + B2) | 50 | 61 |
| B3[a] | 64 | 78 |
| Single X-point (X2 = X3) | 21 | 26 |
| Double X-point (X2 + X3) | 61 | 74 |
| X1 (always present) | 82 | 100 |

[a] When B3 (dZ/dt = 0) was located before the R-peak, it was set to missing.

**Table 3**
Intra class correlation and 95% confidence intervals (95% CI) between the RB and RX intervals measured using ICG (Fig. 5) and the RB and RX intervals from TTE (Fig. 4) for the different candidate B- and X-points.

| | Subjects with multiple B- (*N* = 50) or X-points (*N* = 61) | | All subjects (*N* = 82)[a] | |
|---|---|---|---|---|
| | ICC | 95% CI | ICC | 95% CI |
| B1 | 0.53 | 0.29; 0.70 | 0.48 | 0.27; 0.65 |
| B2 | 0.12 | − 0.08; 0.34 | 0.11 | − 0.06; 0.29 |
| B3 | 0.28 | − 0.13; 0.53 | 0.25 | 0.15; 0.46 |
| X1 | 0.64 | 0.46; 0.76 | 0.63 | 0.48; 0.75 |
| X2 | 0.95 | 0.86; 0.98 | 0.86 | 0.76; 0.91 |
| X3 | 0.50 | − 0.04; 0.83 | 0.55 | − 0.09; 0.82 |

[a] For subjects with no ambiguity B1=B2 and/or X1 = X2 = X3.

**Table 4**
Intra class correlation between the RB interval, RX interval and LVET measured in the ICG and by TTE in the independent replications sets.

Healthy Controls (replication set 1)

| | N | ICC | 95% CI |
|---|---|---|---|
| B point | 35 | 0.50 | 0.22; 0.70 |
| X point | 37 | 0.84 | 0.59; 0.93 |
| PEP | 35 | 0.57 | 0.27; 0.76 |
| LVET | 37 | 0.69 | 0.27; 0.86 |

ConHD patients (replication set 2)

| | N | ICC | 95% CI |
|---|---|---|---|
| B point | 64 | 0.48 | 0.25; 0.66 |
| X point | 65 | 0.82 | 0.48; 0.92 |
| PEP | 64 | 0.50 | 0.22; 0.67 |
| LVET | 64 | 0.59 | 0.10; 0.80 |

Note. PEP = pre ejection period. LVET = left ventricular ejection time.

of the aortic valve.

For the X-point, the best agreement across all subjects was found for candidate X2 (Table 3; ICC = 0.86 95%CI:0.76;0.91). The X2 point also performed best in the subset of subjects with ambiguous X-points. Often, X2 and X3 co-occur, as part of a W-shaped (double U) waveform. Here, we found that the trough in the first U has the best correspondence to the closure of the valve in the echocardiogram. In replication set 1 (healthy controls), ICC for the RX interval based on X2 was 0.84 (Table 4; 95%CI: 0.59; 0.93) and in replication set 2 (patient group) 0.82 (table 4; 95%CI:0.48;0.92).

We also computed the percentages of the candidate X points that fell into the physiological plausible X-point window for each of the X-point candidates. Both X2 and X3 fell 100% of the subjects within this window, but X1 was outside the window in 13.1% of the subjects. Of note, 100% of the 'true' X points measured by TTE fell into this window. On average, the X2-point fell 91 ± 20 ms after T-wave peak.

#### 3.2.3. PEP, and LVET

PEP is defined as the time delay between the ventricular depolarization of the ventricles (Q wave in the ECG) and the start of left ventricular ejection. Because Q-onset was hard to detect in the echocardiographic ECG, $PEP_{TTE}$ was measured from R-onset to the onset of left ventricular ejection. $PEP_{ICG}$ was therefore also measured from R-onset to the B-point. The agreement between $PEP_{ICG}$ and $PEP_{TTE}$ was moderate: ICC = 0.57 in replication set 1, ICC = 0.50 in replication set 2 (see Table 4). Using the optimal B- and X–point candidates, agreement between the LVET from ICG and LVET from TTE was 0.69 (table 4; 95%CI:0.27;0.86) in replication set of healthy children and 0.59 (table 4; 95%CI:0.10;0.80) in the patient replication set. Pearson correlation between ICG and TTE for PEP and LVET in the entire group of subjects was $r = 0.62$ ($p < 0.001$) and $r = 0.80$ ($p < 0.001$) respectively.

## 4. Study 2 (tailoring the Kubicek SV equation to spot electrodes)

### 4.1. Methods

#### 4.1.1. Transthoracic echocardiogram

Stroke volume was assessed in three ways in the echocardiogram; 1. Velocity time integral ($SV_{VTI}$), 2. Biplane method ($SV_{biplane}$) and 3. Three-Dimensional echocardiography ($SV_{3D}$). $SV_{VTI}$ was obtained by multiplying the aortic cross sectional area with the velocity time integral from a pulsed wave Doppler flow signal over the left ventricular outflow tract in a parasternal 5 chamber view. $SV_{biplane}$ was obtained on a 2D view by drawing the end-systolic and end-diastolic left endocardial contours in a 2- and 4 chamber parasternal view and subtracting end-systolic from end-diastolic volumes (modified Simpson method). $SV_{3D}$ was conducted by subtracting end-systolic from end-diastolic volumes (calculated by the use of the divergence Theorem (Goldman, 1991)). Additionally, an average SV ($SV_{average}$) was calculated for every subject across the three methods.

#### 4.1.2. Optimizing stroke volume estimation

Stroke volume was estimated from the ICG using the optimal scoring method for B, C and X points. $dZ/dt_{max}$ was measured in relation to the dZ/dt = 0 line. For every subject in the discovery set, a corrected $Z_0$ was calculated by rearranging the Kubicek equation and filling in the 'true' SV measured by the echocardiogram ($SV_{TTE}$)

$$Z_{0\ corrected} = \sqrt{\frac{\rho L^2 \left(\frac{dZ}{dt}\right)_{max} LVET}{SV_{TTE}}} \quad (2)$$

Subsequently, we tested whether we could successfully predict this corrected $Z_0$ from known subject characteristics (actual $Z_0$, $dZ/dt_{max}$, gender, age, height, weight, BMI, blood pressure and L). This was repeated for the $SV_{TTE}$ obtained with the three different echocardiographic methods ($SV_{biplane}$, $SV_{VTI}$ and $SV_{3D}$) and we also computed a mean SV across these three methods ($SV_{average}$). This provided an intercept and beta-values for regression equations to obtain the corrected $Z_0$ for every echocardiographic method and $SV_{average}$. The resulting regression equations for the corrected $Z_0$ were subsequently applied to the replication sets and the agreement between the SV estimated by ICG (using the estimated corrected $Z_0$) and $SV_{TTE}$ was calculated as an ICC.

**Table 5**
Intra Class Correlations of three different stroke volume measurements from TTE (Biplane, VTI and 3D).

| | Controls | 95%CI | Patients | 95%CI |
|---|---|---|---|---|
| Biplane vs. VTI | 0.57 | − 0.01; 0.81 | 0.35 | − 0.10; 0.68 |
| Biplane vs. 3D | 0.81 | 0.73; 0.87 | 0.71 | 0.54; 0.83 |
| VTI vs. 3D | 0.68 | − 0.02; 0.88 | 0.25 | − 0.10; 0.56 |

#### 4.1.3. Statistical analyses

IBM SPSS statistics software (version 23.0, Armonk, NY) was used for statistical analysis. Multiple regression analysis (backward method) was used to find the optimal regression equation for the corrected $Z_0$.

### 4.2. Results

Agreement between the SV obtained with the three different TTE methods is shown in Table 5. The optimal regression equation for $Z_{0\ corrected}$ was calculated for every SV calculation method separately ($SV_{biplane}$, $SV_{VTI}$, $SV_{3D}$ and $SV_{average}$) and shown in Table 6. The ratio between the calculated $Z_{0\ corrected}$ and the measured $Z_0$ was on average 1.36 ± 0.26. Simply using a corrected $Z_0$ based on this ratio yielded ICCs that were always higher than the uncorrected SV but 4 to 56% lower than those using our equation with dZ/dt (data not shown). In the discovery set, the agreement between the uncorrected SV from ICG and the SV from the echocardiogram was low to moderate (Table 7). When employing the corrected $Z_0$, agreement between SV from ICG and SV from echocardiography strongly increased. In the independent replication set, the median ICC across different TTE methods increased from 0.22 to 0.70 in the healthy controls and from 0.14 to 0.37 in the ConHD patients. In addition to the ICCs, Pearson correlations were calculated in order to facilitate comparison to different studies as most other studies report only the correlation. Finally, bias, 95% limits of agreement and mean absolute percentage error are shown in Table 8 and Fig. 7 shows the Bland-Altman plot and SV from ICG against SV from TTE for $SV_{average}$.

## 5. Discussion

The aim of this study was to improve SV assessment from spot-electrode based ICG in a pediatric population of both healthy children and children with a corrected ConHD. We tackled two sources of error in SV estimation: (1) ambiguity of the scoring of the B- C– and X-points, (2) the use of the Kubicek formula uncorrected for spot-band differences in baseline thorax impedance and uncorrected for the reduction in thorax volume enclosed by the measuring electrodes.

**Table 6**
Regression equations for the corrected $Z_0$ using the stroke volume measured by the three TTE and their average. Last column shows the explained variance of the regression.

| | $Z_{0\ corrected}$ | $R^2$ |
|---|---|---|
| $SV_{biplane}$ | $-1.291 + 0.304 * Z_0 - 6.695 * dZdt_{max} + 0.442 * L$ | 0.65 |
| $SV_{VTI}$ | $4.619 + 0.227 * Z_0 - 5.363 * dZdt_{max}$ | 0.71 |
| $SV_{3D}$ | $7.978 - 6.359 * dZdt_{max}$ | 0.65 |
| $SV_{average}$ | $7.337 - 6.208 * dZdt_{max}$ | 0.70 |

**Table 7**
Intra Class Correlations (ICC), Pearson correlations (r) between SV estimated by ICG ($SV_{ICG}$) using the regression equation for the corrected $Z_0$ -specific to the SV method- and the SV measured by TTE ($SV_{TTE}$) for the discovery and replication sets. Final columns show mean $SV_{TTE}$ and $SV_{ICG}$ (corrected and uncorrected).

| | | $ICC_{uncorrected}$ | $ICC_{corrected}$ | r | $SV_{ICG\ uncorrected}$ (ml) | $SV_{ICG\ corrected}$ (ml) | $SV_{TTE}$ (ml) |
|---|---|---|---|---|---|---|---|
| $SV_{biplane}$ | Discovery | 0.22 (95%CI: − 0.08;0.48) | 0.79 (95%CI:0.68;0.86) | 0.81 ($p < 0.001$) | 86.1 ± 51.4 | 34.9 ± 12.7 | 35.4 ± 16.2 |
| | Controls | 0.17 (95%CI: − 0.09;0.45) | 0.68 (95%CI:0.38;0.80) | 0.68 ($p < 0.001$) | 88.5 ± 51.8 | 37.0 ± 12.9 | 37.4 ± 17.4 |
| | Patients | 0.14 (95%CI: − 0.08;0.37) | 0.36 (95%CI:0.08;0.59) | 0.50 ($p < 0.001$) | 94.7 ± 44.0 | 39.7 ± 9.8 | 48.1 ± 16.6 |
| $SV_{VTI}$ | Discovery | 0.48 (95%CI:0.03;0.73) | 0.88 (95%CI:0.81;0.92) | 0.89 ($p < 0.001$) | 86.1 ± 51.4 | 54.9 ± 29.0 | 52.0 ± 25.9 |
| | Controls | 0.44 (95%CI:0.02;0.71) | 0.81 (95%CI:0.63;0.90) | 0.90 ($p < 0.001$) | 88.5 ± 51.8 | 61.5 ± 31.9 | 53.8 ± 23.5 |
| | Patients | 0.15 (95%CI:0.08;0.36) | 0.28 (95%CI:0.05;0.49) | 0.32 ($p = 0.010$) | 94.7 ± 44.0 | 64.5 ± 21.7 | 75.8 ± 26.5 |
| $SV_{3D}$ | Discovery | 0.22 (95%CI: − 0.09;0.50) | 0.80 (95%CI:0.69;0.87) | 0.81 ($p < 0.001$) | 86.1 ± 51.4 | 40.3 ± 20.8 | 40.6 ± 17.9 |
| | Controls | 0.16 (95%CI: − 0.10;0.44) | 0.60 (95%CI:0.32;0.78) | 0.66 ($p < 0.001$) | 88.5 ± 51.8 | 45.4 ± 22.8 | 41.4 ± 18.5 |
| | Patients | 0.01 (95%CI: − 0.0;0.30) | 0.42 (95%CI:0.17;0.62) | 0.43 ($p = 0.001$) | 94.7 ± 44.0 | 48.0 ± 16.1 | 46.3 ± 12.9 |
| $SV_{average}$ | Discovery | 0.33 (95%CI: − 0.07;0.61) | 0.86 (95%CI:0.80;0.91) | 0.88 ($p < 0.001$) | 86.1 ± 51.4 | 45.2 ± 23.4 | 42.2 ± 19.3 |
| | Controls | 0.26 (95%CI: − 0.08;0.56) | 0.72 (95%CI:0.50;0.85) | 0.82 ($p < 0.001$) | 88.5 ± 51.8 | 50.9 ± 25.6 | 44.1 ± 18.6 |
| | Patients | 0.13 (95%CI: − 0.07;0.33) | 0.37 (95%CI:0.14;0.56) | 0.38 ($p = 0.001$) | 94.7 ± 44.0 | 53.4 ± 17.9 | 57.9 ± 16.9 |

**Table 8**
Bias, 95% limits of agreement and MAPE for the different methods. Bias is calculated as: $SV_{TTE}$-$SV_{ICG}$ (ml). MAPE = mean absolute percentage error.

| Healthy controls (replication set 1) | | | | |
|---|---|---|---|---|
| | Mean $SV_{ICG}$ (ml) | Bias (ml) | 95% limits of agreement | MAPE (%) |
| $SV_{biplane}$ | 37.01 | − 6.95 | − 21.12; 22.79 | 23.88 |
| $SV_{VTI}$ | 61.48 | − 6.95 | − 37.62; 23.72 | 20.93 |
| $SV_{3D}$ | 45.38 | − 5.93 | − 40.22; 28.35 | 31.61 |
| $SV_{average}$ | 50.88 | − 6.14 | − 36.14; 23.86 | 23.86 |
| ConHD patients (replication set 2) | | | | |
| $SV_{biplane}$ | 39.70 | 8.99 | − 19.62; 37.61 | 22.50 |
| $SV_{VTI}$ | 64.45 | 12.01 | − 44.24; 68.78 | 26.92 |
| $SV_{3D}$ | 47.96 | − 0.44 | − 31.11; 30.24 | 22.97 |
| $SV_{average}$ | 53.72 | 4.59 | − 33.90; 43.09 | 21.83 |

As a first step (study 1), scoring of the landmarks in the ICG defining the systolic time intervals was optimized in a discovery set (70% of the total dataset of healthy controls). In case of a biphasic C wave, the first peak was chosen based on the visual inspection of the echocardiogram in which it was clear that the moment of maximal blood flow acceleration in the aorta is always very soon after opening of the aortic valve. For the B-point (opening of the aortic valve), the point before the highest upstroke showed best agreement with echocardiography (B1 in the lower panel of Fig. 1). For the X-point (closing of the aortic valve) the first trough (X2 in the lower panel of Fig. 1) showed best agreement. Additionally, point X2 showed the highest percentage of beats falling into the physiological plausible X-window. Criterion validity for the optimized scoring method was obtained from two independent replication sets; replication set 1: the remaining 30% of the healthy controls and replication set 2: a group of patients operated for their ConHD. In replication set 1, agreement was moderate to good (ICC B-point = 0.50; X-point = 0.84) and comparable results were found in the patient group (ICC B-point = 0.48; X-point = 0.82).

After optimizing the scoring of the B- C– and X-point in the ICG, we calculated a corrected $Z_0$ in the discovery set by filling in the 'true' SV from the simultaneously recorded echocardiogram into the Kubicek formula (study 2). This allowed us to estimate an ICG-based SV that is applicable for spot electrodes which are now common in both laboratory and ambulatory applications. The simple formula used for $Z_0$ correction can eliminate the differences in baseline values of Z0 and the distance between measuring electrodes existing between the spot and band configurations. In the discovery set, the corrected $Z_0$ was best estimated by a regression equation including electrode distance and/or $dZdt_{max}$ as predictors. Thus, interestingly, the actual $Z_0$ was removed from the equation. Removing $Z_0$ from the SV estimation equation solves any problems related to the sensitivity of baseline thorax impedance to electrode type and placement. Our results are well-aligned with previous applications of ICG based CO-estimation without baseline thorax impedance (Payseur et al., 2016; Ebrahim et al., 2016). Of note, however, is that under anaesthesia ICG-based CO estimation does not seem reliable (Taylor et al., 2011; Taylor et al., 2012).

We tested our improved SV assessment methods in two independent replication sets and showed moderate to good agreement for SV in healthy controls after correction (median ICC 0.70) but low to moderate in ConHD patients (median ICC 0.37). In the healthy controls, highest ICC for SV was obtained when applying the $Z_0$ corrected for $SV_{VTI}$. However, since there is no consensus favouring one method over another, we advise to use $Z_0$ corrected for $SV_{average}$ when estimating SV from ICG using spot electrodes in healthy subjects ($Z_0$ corrected = $7.337–6.208 * dZdt_{max}$). The agreement found between $SV_{ICG}$ and $SV_{TTE}$ was always lower in patients compared to healthy controls. This was not surprising since the agreement between different methods of measuring stroke volume with TTE was also always lower in patients compared to controls. Of note, $SV_{VTI}$ may have been biased in patients with CoA as they often -approximately 2/3 of patients- have a bicuspid valve which may make the velocity time integral method less reliable. Therefore, we advise to use the corrected $Z_0$ for $SV_{3D}$ ($Z_0$ corrected = $7.978–6.359 * dZdt_{max}$) in patients since this closely resembles that of $SV_{average}$ but not included the potentially biased $SV_{VTI}$. Also, this correction gains the highest ICC in patients (Table 7).

Although we here focus on SV estimation, ICG has also been widely used to noninvasively measure cardiac sympathetic activity by its effect on contractility (Cybulski et al., 2004; Newlin and Levenson, 1979; Berntson et al., 1994). Increased activity of the sympathetic branch of the autonomic nervous system to the heart is a powerful mechanism to compensate for altered hemodynamics due to heart disease, but it may in time have detrimental effects to the myocardium (Mancia et al., 1999; Mann et al., 1992; Packer, 1992b; Packer, 1992a). Enhanced

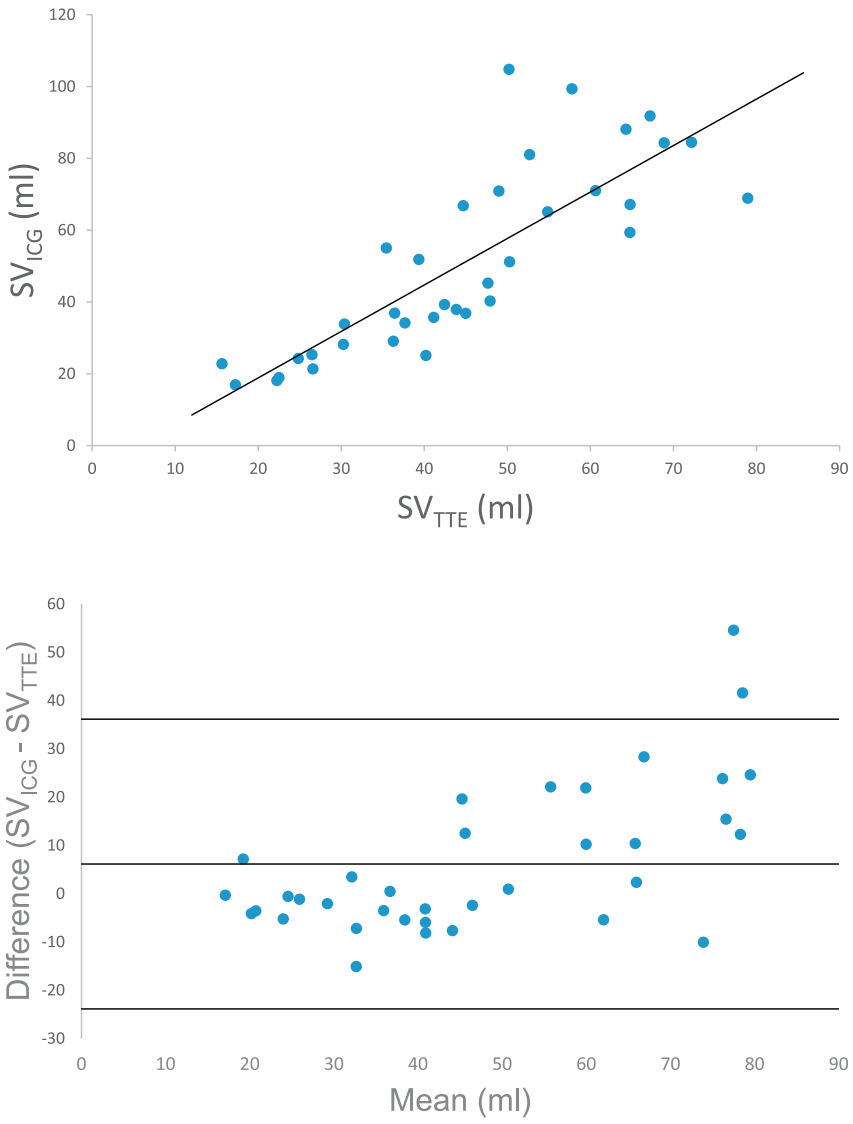


**Fig. 7.** $SV_{average}$ from TTE plotted against SV from ICG (upper panel) and Bland- Altman plot (lower panel) for $SV_{average}$ in replication set 1.

sympathetic cardiac nervous activity is an important factor in the progression of heart failure and may also play a crucial role in the long term sequelae in ConHD patients (Nederend et al., 2016). Studies comparing cardiac sympathetic activity in ConHD patients with healthy controls could help explain how late cardiac complications arise in ConHD, particularly if these studies could be done in real life settings as various studies have reported reduced exercise tolerance and functional status as reflected in reduced capacity to deal with activities of daily living (Muller et al., 2009; Kempny et al., 2012).

There are several methods to measure cardiac sympathetic activity; e.g. scintigraphy of radiolabelled metaiodobenzylguanidine, measurement of norepinephrine regional spill over of plasma catecholamines, microneurography and pharmacological blockade (de Geus et al., 2015; Grassi and Esler, 1999). Changes in PEP co-vary strongly with changes in contractility which led to the use of a change in PEP as a measure of the change in cardiac sympathetic activity (Newlin and Levenson, 1979; Berntson et al., 1994; de Geus and Van Doornen, 1996; Harris et al., 1967; Kupper et al., 2006; Richter and Gendolla, 2009).

This study found moderate agreement for PEP measured using TTE and ICG in healthy children (ICC = 0.57, Table 4) and ConHD patients (ICC = 0.50, table 4). LVET showed good agreement between ICG and TTE (ICC = 0.69) in healthy children, and moderate agreement (ICC = 0.59) in patients. In the entire group of subjects, Pearson correlation between ICG and TTE for PEP and LVET was $r = 0.62$ ($p < 0.001$) and $r = 0.80$ ($p < 0.001$) respectively. This is in accordance with a recent study by Lorne et al. comparing LVET measured by transoesophageal echocardiography and ICG (Lorne et al., 2014) who found good agreement for LVET ($r = 0.69$) as did Cybulski et al. who compared systolic time intervals between TTE and ICG and found good agreement for PEP ($r = 0.73$) and LVET ($r = 0.84$) in young adults in supine and tilted position (Cybulski et al., 2004). The correlations for PEP and LVET found in our study were lower for PEP ($r = 0.62$ for the entire group, $N = 183$) and comparable for LVET ($r = 0.80$ for the entire group, $N = 191$). However, Fellahi et al. found only a weak agreement between LVET ($r = 0.27$) measured by TTE and ICG (Fellahi et al., 2009) and Carvallo et al. conclude that ICG was inaccurate is assessing PEP ($r = 0.54$–$0.75$ for different scoring methods) and LVET ($r = 0.19$–$0.36$) compared to TTE (Carvalho et al., 2010).

A limitation of this study is that echocardiography and ICG were only measured in a supine position during rest. Therefore, it is unclear how the agreement is in different body positions and at higher heart rates. However, Welsman et al. and Pianosi et al. found increasing CO measured by ICG during a graded exercise test in children/young adults as expected, suggesting that ICG derived CO is able to detect changes in CO with changing physical activity (Welsman et al., 2005; Pianosi, 2004). Also, the current study used transthoracic echocardiography as a gold standard for SV measurement while this method itself has its own inaccuracy and therefore introduces additional error in the comparison

(Cecconi et al., 2009). This is also reflected in Table 5; agreement between the different methods for SV calculation is not perfect – especially in patients. In a meta-analysis Critchley et al. found an overall percentage error of 65% (25–225%) for Doppler methods compared to 37% (15–82%) for impedance (Critchley and Critchley, 1999). Likewise, Chew et al. found an average error of around 30% (Chew and Poelaert, 2003). Taken that into account, the results of this study are satisfactory. SV assessed by the use of ICG is non-inferior to other modalities available and therefore usable in pediatric populations. The fact that ICG is non-invasive and can be measured ambulatory is an important advantage of this method. However, caution is warranted when employing ICG in cardiac patients, as the reliability is less compared to healthy cohorts as shown in the current and other (Raaijmakers et al., 1999) studies. This, may be less of an issue for within-participant contrasts, but could strongly bias comparisons between groups. Further caution is required when different electrode configurations are used. It has been shown that the validity of the Kubicek equation is sensitive to the exact electrode configuration (van der Meer et al., 1996) and we fully suspect that this remains true when using our new dZ/dt approach.

In conclusion, SV estimation by ICG showed moderate to good agreement in healthy children after adjustment of the Kubicek equation. When using spot electrodes, it is advised to use an adjusted Kubicek equation. In pediatric patients, agreement was slight to moderate. Stroke volume assessed by the use of ICG is non-inferior to other modalities available and therefore usable in pediatric populations. Additionally, it has the advantage of measurement in an ambulatory setting, which may increase clinical relevance. However, validity is somewhat less in patients compared to healthy controls. Therefore, ICG should be used as an addition to the clinical evaluation and cannot replace standard SV measurement in cardiac patients. Comparison of systolic time intervals including PEP and LVET measured by ICG and transthoracic echocardiography simultaneously, revealed moderate agreement in healthy children and pediatric ConHD patients. Agreement was somewhat better in healthy children, especially in the case of LVET. A next step would be to relate ambulatory recorded SV, CO and cardiac sympathetic activity to clinical features in order to unravel the role of these parameters in the etiology of ConHD and to establish whether non-invasive ambulatory ICG might be of additional value in the clinical evaluation of pediatric cardiac patients.

## Acknowledgements

The authors thank Gwen C. Bos, Fransisca P. de Klerk-Voll and Eveline M. Ligthart of the Department of Pediatric Echocardiography, Leiden University Medical Center for the help in making the echocardiographs.

## Funding

This work was supported by the VU-AMS fund.

## References

Berntson, G.G., Cacioppo, J.T., Binkley, P.F., Uchino, B.N., Quigley, K.S., Fieldstone, A., 1994. Autonomic cardiac control. III. Psychological stress and cardiac response in autonomic space as revealed by pharmacological blockades. Psychophysiology 31, 599–608.

Blohm, M.E., Obrecht, D., Hartwich, J., Mueller, G.C., Kersten, J.F., Weil, J., Singer, D., 2014. Impedance cardiography (electrical velocimetry) and transthoracic echocardiography for non-invasive cardiac output monitoring in pediatric intensive care patients: a prospective single-center observational study. Crit. Care 18, 603.

Boomsma, D.I., de Vries, J., Orlebeke, J.F., 1989. Comparison of spot and band impedance cardiogram electrodes across different tasks. Psychophysiology 26, 695–699.

Bouchardy, J., Therrien, J., Pilote, L., Ionescu-Ittu, R., Martucci, G., Bottega, N., Marelli, A.J., 2009. Atrial arrhythmias in adults with congenital heart disease. Circulation 120, 1679–1686.

Brown, C.V., Martin, M.J., Shoemaker, W.C., Wo, C.C., Chan, L., Azarow, K., Demetriades, D., 2005. The effect of obesity on bioimpedance cardiac index. Am. J. Surg. 189, 547–550.

Carvalho, P., Paiva, R.P., Couceiro, R., Henriques, J., Antunes, M., Quintal, I., Muehlsteff, J., Aubert, X., 2010. Comparison of systolic time interval measurement modalities for portable devices. Conf. Proc. IEEE Eng. Med. Biol. Soc. 2010, 606–609.

Cecconi, M., Rhodes, A., Poloniecki, J., Della, R.G., Grounds, R.M., 2009. Bench-to-bedside review: the importance of the precision of the reference technique in method comparison studies–with specific reference to the measurement of cardiac output. Crit. Care 13, 201.

Charloux, A., Lonsdorfer-Wolf, E., Richard, R., Lampert, E., Oswald-Mammosser, M., Mettauer, B., Geny, B., Lonsdorfer, J., 2000. A new impedance cardiograph device for the non-invasive evaluation of cardiac output at rest and during exercise: comparison with the "direct" Fick method. Eur. J. Appl. Physiol. 82, 313–320.

Chew, M.S., Poelaert, J., 2003. Accuracy and repeatability of pediatric cardiac output measurement using Doppler: 20-year review of the literature. Intensive Care Med. 29, 1889–1894.

Critchley, L.A., Critchley, J.A., 1999. A meta-analysis of studies using bias and precision statistics to compare cardiac output measurement techniques. J. Clin. Monit. Comput. 15, 85–91.

Cybulski, G., Michalak, E., Kozluk, E., Piatkowska, A., Niewiadomski, W., 2004. Stroke volume and systolic time intervals: beat-to-beat comparison between echocardiography and ambulatory impedance cardiography in supine and tilted positions. Med. Biol. Eng. Comput. 42, 707–711.

de Geus, E.J., Van Doornen, L.J., 1996. Ambulatory assessment of parasympathetic/sympathetic balance by impedance cardiography. In: Fahrenberg, J.M.M. (Ed.), Ambulatory Assessment: Computer-Assisted Psychological and Psychophysiological Methods in Monitoring and Field Studies. Gottingen, Germany, Hogrefe & Huber, pp. 141–163.

de Geus, E.J., Willemsen, G.H., Klaver, C.H., Van Doornen, L.J., 1995. Ambulatory measurement of respiratory sinus arrhythmia and respiration rate. Biol. Psychol. 41, 205–227.

de Geus, E.J., van Lien, R., Neijts, M., Willemsen, 2015. Genetics of autonomic nervous system activity. In: The Oxford Handbook of Molecular Psychology. Oxford University Press, pp. 357–390.

Doering, L., Lum, E., Dracup, K., Friedman, A., 1995. Predictors of between-method differences in cardiac output measurement using thoracic electrical bioimpedance and thermodilution. Crit. Care Med. 23, 1667–1673.

Ebrahim, M., Hegde, S., Printz, B., Abcede, M., Proudfoot, J.A., Davis, C., 2016. Evaluation of impedance cardiography for measurement of stroke volume in congenital heart disease. Pediatr. Cardiol.

Engelfriet, P.M., Duffels, M.G., Moller, T., Boersma, E., Tijssen, J.G., Thaulow, E., Gatzoulis, M.A., Mulder, B.J., 2007. Pulmonary arterial hypertension in adults born with a heart septal defect: the euro heart survey on adult congenital heart disease. Heart 93, 682–687.

Engoren, M., Barbee, D., 2005. Comparison of cardiac output determined by bioimpedance, thermodilution, and the Fick method. Am. J. Crit. Care 14, 40–45.

Ermishkin, V.V., Kolesnikov, V.A., Lukoshkova, E.V., 2014. Age-dependent and 'pathologic' changes in ICG waveforms resulting from superposition of pre-ejection and ejection waves. Physiol. Meas. 35, 943–963.

Fellahi, J.L., Caille, V., Charron, C., Deschamps-Berger, P.H., Vieillard-Baron, A., 2009. Noninvasive assessment of cardiac index in healthy volunteers: a comparison between thoracic impedance cardiography and Doppler echocardiography. Anesth. Analg. 108, 1553–1559.

Fuller, H.D., 1992. The validity of cardiac output measurement by thoracic impedance: a meta-analysis. Clin. Invest. Med. 15, 103–112.

Goedhart, A.D., Kupper, N., Willemsen, G., Boomsma, D.I., de Geus, E.J., 2006. Temporal stability of ambulatory stroke volume and cardiac output measured by impedance cardiography. Biol. Psychol. 72, 110–117.

Goedhart, A.D., van der Sluis, S., Houtveen, J.H., Willemsen, G., de Geus, E.J., 2007. Comparison of time and frequency domain measures of RSA in ambulatory recordings. Psychophysiology 44, 203–215.

Goldman, R.N., 1991. Area of Planar Polygons and Volume of Polyhedra. Graphics Gems II.

Grassi, G., Esler, M., 1999. How to assess sympathetic activity in humans. J. Hypertens. 17, 719–734.

Grollmuss, O., Demontoux, S., Capderou, A., Serraf, A., Belli, E., 2012. Electrical velocimetry as a tool for measuring cardiac output in small infants after heart surgery. Intensive Care Med. 38, 1032–1039.

Harris, W.S., Schoenfeld, C.D., Weissler, A.M., 1967. Effects of adrenergic receptor activation and blockade on the systolic preejection period, heart rate, and arterial pressure in man. J. Clin. Invest. 46, 1704–1714.

Houtveen, J.H., Groot, P.F., de Geus, E.J., 2006. Validation of the thoracic impedance derived respiratory signal using multilevel analysis. Int. J. Psychophysiol. 59, 97–106.

Kamath, S.A., Drazner, M.H., Tasissa, G., Rogers, J.G., Stevenson, L.W., Yancy, C.W., 2009. Correlation of impedance cardiography with invasive hemodynamic measurements in patients with advanced heart failure: the BioImpedance CardioGraphy (BIG) substudy of the evaluation study of congestive heart failure and pulmonary artery catheterization effectiveness (ESCAPE) trial. Am. Heart J. 158, 217–223.

Kelsey, R.M., Guethlein, W., 1990. An evaluation of the ensemble averaged impedance cardiogram. Psychophysiology 27, 24–33.

Kempny, A., Dimopoulos, K., Uebing, A., Moceri, P., Swan, L., Gatzoulis, M.A., Diller, G.P., 2012. Reference values for exercise limitations among adults with congenital heart disease. Relation to activities of daily life–single centre experience and review of published data. Eur. Heart J. 33, 1386–1396.

Kemps, H.M., Thijssen, E.J., Schep, G., Sleutjes, B.T., De Vries, W.R., Hoogeveen, A.R., Wijn, P.F., Doevendans, P.A., 2008. Evaluation of two methods for continuous

cardiac output assessment during exercise in chronic heart failure patients. J. Appl. Physiol. 105 (1985), 1822–1829.
Kubicek, W.G., Karnegis, J.N., Patterson, R.P., Witsoe, D.A., Mattson, R.H., 1966. Development and evaluation of an impedance cardiac output system. Aerosp. Med. 37, 1208–1212.
Kupper, N., Willemsen, G., Boomsma, D.I., de Geus, E.J., 2006. Heritability of indices for cardiac contractility in ambulatory recordings. J. Cardiovasc. Electrophysiol. 17, 877–883.
Lababidi, Z., Ehmke, D.A., Durnin, R.E., Leaverton, P.E., Lauer, R.M., 1970. The first derivative thoracic impedance cardiogram. Circulation 41, 651–658.
Lorne, E., Mahjoub, Y., Diouf, M., Sleghem, J., Buchalet, C., Guinot, P.G., Petiot, S., Kessavane, A., Dehedin, B., Dupont, H., 2014. Accuracy of impedance cardiography for evaluating trends in cardiac output: a comparison with oesophageal Doppler. Br. J. Anaesth. 113, 596–602.
Lozano, D.L., Norman, G., Knox, D., Wood, B.L., Miller, B.D., Emery, C.F., Berntson, G.G., 2007. Where to B in dZ/dt. Psychophysiology 44, 113–119.
Mancia, G., Grassi, G., Giannattasio, C., Seravalle, G., 1999. Sympathetic activation in the pathogenesis of hypertension and progression of organ damage. Hypertension 34, 724–728.
Mann, D.L., Kent, R.L., Parsons, B., Cooper, G., 1992. Adrenergic effects on the biology of the adult mammalian cardiocyte. Circulation 85, 790–804.
Marik, P.E., 2013. Noninvasive cardiac output monitors: a state-of the-art review. J. Cardiothorac. Vasc. Anesth. 27, 121–134.
Miles, D.S., Gotshall, R.W., 1989. Impedance cardiography: noninvasive assessment of human central hemodynamics at rest and during exercise. Exerc. Sport Sci. Rev. 17, 231–263.
Moons, P., Bovijn, L., Budts, W., Belmans, A., Gewillig, M., 2010. Temporal trends in survival to adulthood among patients born with congenital heart disease from 1970 to 1992 in Belgium. Circulation 122, 2264–2272.
Morgan, B.E., Horn, A.R., Bergman, N.J., 2011. Should neonates sleep alone? Biol. Psychiatry 70, 817–825.
Muller, J., Christov, F., Schreiber, C., Hess, J., Hager, A., 2009. Exercise capacity, quality of life, and daily activity in the long-term follow-up of patients with univentricular heart and total cavopulmonary connection. Eur. Heart J. 30, 2915–2920.
Nederend, I., Jongbloed, M.R.M., de Geus, E.J., Blom, N.A., ten Harkel, A.D.J., 2016. Postnatal cardiac autonomic nervous control in pediatric congenital heart disease. J. Cardiovasc. Dev. Dis. 3.
Neijts, M., van Lien, R., Kupper, N., Boomsma, D., Willemsen, G., de Geus, E.J., 2015. Heritability and temporal stability of ambulatory autonomic stress reactivity in unstructured 24-h recordings. Psychosom. Med (In press).
Newlin, D.B., Levenson, R.W., 1979. Pre-ejection period: measuring beta-adrenergic influences upon the heart. Psychophysiology 16, 546–553.
Noori, S., Drabu, B., Soleymani, S., Seri, I., 2012. Continuous non-invasive cardiac output measurements in the neonate by electrical velocimetry: a comparison with echocardiography. Arch. Dis. Child. Fetal Neonatal Ed. 97, F340–F343.
Norozi, K., Beck, C., Osthaus, W.A., Wille, I., Wessel, A., Bertram, H., 2008. Electrical velocimetry for measuring cardiac output in children with congenital heart disease. Br. J. Anaesth. 100, 88–94.
Ono, T., Miyamura, M., Yasuda, Y., Ito, T., Saito, T., Ishiguro, T., Yoshizawa, M., Yambe, T., 2004. Beat-to-beat evaluation of systolic time intervals during bicycle exercise using impedance cardiography. Tohoku J. Exp. Med. 203, 17–29.
Packer, M., 1992a. Pathophysiology of chronic heart failure. Lancet 340, 88–92.
Packer, M., 1992b. The neurohormonal hypothesis: a theory to explain the mechanism of disease progression in heart failure. J. Am. Coll. Cardiol. 20, 248–254.
Payseur, J.D., Rigney, J.J., Turner, S.L., Wu, X., Murphy, D.J., Rossman, E.I., 2016. Evaluation of a method utilizing PhysioFlow(R), a novel signal morphology-based form of impedance cardiography, to measure cardiac output in the conscious beagle. J. Pharmacol. Toxicol. Methods.
Penney, B.C., Patwardhan, N.A., Wheeler, H.B., 1985. Simplified electrode array for impedance cardiography. Med. Biol. Eng. Comput. 23, 1–7.
Peyton, P.J., Chong, S.W., 2010. Minimally invasive measurement of cardiac output during surgery and critical care: a meta-analysis of accuracy and precision. Anesthesiology 113, 1220–1235.
Pianosi, P.T., 2004. Measurement of exercise cardiac output by thoracic impedance in healthy children. Eur. J. Appl. Physiol. 92, 425–430.
Qu, M.H., Zhang, Y.J., Webster, J.G., Tompkins, W.J., 1986. Motion artifact from spot and band electrodes during impedance cardiography. IEEE Trans. Biomed. Eng. 33, 1029–1036.
Raaijmakers, E., Faes, T.J., Scholten, R.J., Goovaerts, H.G., Heethaar, R.M., 1999. A meta-analysis of three decades of validating thoracic impedance cardiography. Crit. Care Med. 27, 1203–1213.
Rauch, R., Welisch, E., Lansdell, N., Burrill, E., Jones, J., Robinson, T., Bock, D., Clarson, C., Filler, G., Norozi, K., 2013. Non-invasive measurement of cardiac output in obese children and adolescents: comparison of electrical cardiometry and transthoracic Doppler echocardiography. J. Clin. Monit. Comput. 27, 187–193.
Richard, R., Lonsdorfer-Wolf, E., Charloux, A., Doutreleau, S., Buchheit, M., Oswald-Mammosser, M., Lampert, E., Mettauer, B., Geny, B., Lonsdorfer, J., 2001. Non-invasive cardiac output evaluation during a maximal progressive exercise test, using a new impedance cardiograph device. Eur. J. Appl. Physiol. 85, 202–207.
Richter, M., Gendolla, G.H., 2009. The heart contracts to reward: monetary incentives and preejection period. Psychophysiology 46, 451–457.
Riese, H., Groot, P.F., van den Berg, M., Kupper, N.H., Magnee, E.H., Rohaan, E.J., Vrijkotte, T.G., Willemsen, G., de Geus, E.J., 2003. Large-scale ensemble averaging of ambulatory impedance cardiograms. Behav. Res. Methods Instrum. Comput. 35, 467–477.
Sagie, A., Larson, M.G., Goldberg, R.J., Bengtson, J.R., Levy, D., 1992. An improved method for adjusting the QT interval for heart rate (the Framingham heart study). Am. J. Cardiol. 70, 797–801.
Schmidt, C., Theilmeier, G., Van, A.H., Korsmeier, P., Wirtz, S.P., Berendes, E., Hoffmeier, A., Meissner, A., 2005. Comparison of electrical velocimetry and transoesophageal Doppler echocardiography for measuring stroke volume and cardiac output. Br. J. Anaesth. 95, 603–610.
Schubert, S., Schmitz, T., Weiss, M., Nagdyman, N., Huebler, M., Alexi-Meskishvili, V., Berger, F., Stiller, B., 2008. Continuous, non-invasive techniques to determine cardiac output in children after cardiac surgery: evaluation of transesophageal Doppler and electric velocimetry. J. Clin. Monit. Comput. 22, 299–307.
Sherwood, A., Allen, M.T., Fahrenberg, J., Kelsey, R.M., Lovallo, W.R., Van Doornen, L.J., 1990. Methodological guidelines for impedance cardiography. Psychophysiology 27, 1–23.
Sherwood, A., Royal, S.A., Hutcheson, J.S., Turner, J.R., 1992. Comparison of impedance cardiographic measurements using band and spot electrodes. Psychophysiology 29, 734–741.
Shoemaker, W.C., Belzberg, H., Wo, C.C., Milzman, D.P., Pasquale, M.D., Baga, L., Fuss, M.A., Fulda, G.J., Yarbrough, K., Van DeWater, J.P., et al., 1998. Multicenter study of noninvasive monitoring systems as alternatives to invasive monitoring of acutely ill emergency patients. Chest 114, 1643–1652.
Summers, R.L., Shoemaker, W.C., Peacock, W.F., Ander, D.S., Coleman, T.G., 2003. Bench to bedside: electrophysiologic and clinical principles of noninvasive hemodynamic monitoring using impedance cardiography. Acad. Emerg. Med. 10, 669–680.
Taylor, K., La, R.G., McCrindle, B.W., Manlhiot, C., Redington, A., Holtby, H., 2011. A comparison of cardiac output by thoracic impedance and direct fick in children with congenital heart disease undergoing diagnostic cardiac catheterization. J. Cardiothorac. Vasc. Anesth. 25, 776–779.
Taylor, K., Manlhiot, C., McCrindle, B., Grosse-Wortmann, L., Holtby, H., 2012. Poor accuracy of noninvasive cardiac output monitoring using bioimpedance cardiography [PhysioFlow(R)] compared to magnetic resonance imaging in pediatric patients. Anesth. Analg. 114, 771–775.
van der Linde, D., Konings, E.E., Slager, M.A., Witsenburg, M., Helbing, W.A., Takkenberg, J.J., Roos-Hesselink, J.W., 2011. Birth prevalence of congenital heart disease worldwide: a systematic review and meta-analysis. J. Am. Coll. Cardiol. 58, 2241–2247.
van der Meer, B.J., Woltjer, H.H., Sousman, A.M., Schreuder, W.O., Bulder, E.R., Huybregts, M.A., de Vries, P.M., 1996. Impedance cardiography. Importance of the equation and the electrode configuration. Intensive Care Med. 22, 1120–1124.
van Dijk, A.E., van Lien, R., van Eijsden, M., Gemke, R.J., Vrijkotte, T.G., de Geus, E.J., 2013. Measuring cardiac autonomic nervous system (ANS) activity in children. J. Vis. Exp. e50073.
van Eijnatten, M.A.J.M., van Rijssel, M.J., Peters, R.J.A., Vereaasdonk, R.M., Meijer, J.H., 2014. Comparison of cardiac time intervals between echocardiography and impedance cardiography at various heart rates. J. Electr. Bioimpedance 5, 2–8.
van Lien, R., Schutte, N.M., Meijer, J.H., de Geus, E.J., 2013. Estimated preejection period (PEP) based on the detection of the R-wave and dZ/dt-min peaks does not adequately reflect the actual PEP across a wide range of laboratory and ambulatory conditions. Int. J. Psychophysiol. 87, 60–69.
van Lien, R., Neijts, M., Willemsen, G., de Geus, E.J., 2014. Ambulatory measurement of the ECG T-wave amplitude. Psychophysiology 52, 225–237.
van Riel, A.C., Schuuring, M.J., van Hessen, I.D., Zwinderman, A.H., Cozijnsen, L., Reichert, C.L., Hoorntje, J.C., Wagenaar, L.J., Post, M.C., van Dijk, A.P., et al., 2014. Contemporary prevalence of pulmonary arterial hypertension in adult congenital heart disease following the updated clinical classification. Int. J. Cardiol. 174, 299–305.
Verheugt, C.L., Uiterwaal, C.S., van der Velde, E.T., Meijboom, F.J., Pieper, P.G., van Dijk, A.P., Vliegen, H.W., Grobbee, D.E., Mulder, B.J., 2010. Mortality in adult congenital heart disease. Eur. Heart J. 31, 1220–1229.
Viskin, S., 2009. The QT interval: too long, too short or just right. Heart Rhythm. 6, 711–715.
Vrijkotte, T.G., Van Doornen, L.J., de Geus, E.J., 2004. Overcommitment to work is associated with changes in cardiac sympathetic regulation. Psychosom. Med. 66, 656–663.
Walsh, E.P., Cecchin, F., 2007. Arrhythmias in adult patients with congenital heart disease. Circulation 115, 534–545.
Warnes, C.A., Williams, R.G., Bashore, T.M., Child, J.S., Connolly, H.M., Dearani, J.A., del Nido, Pedro, Fasules, J.W., Graham Jr., T.P., Hijazi, Z.M., et al., 2008. ACC/AHA 2008 guidelines for the management of adults with congenital heart disease: a report of the American College of Cardiology/American Heart Association Task Force on Practice Guidelines (Writing Committee to Develop Guidelines on the Management of Adults With Congenital Heart Disease). Developed in Collaboration With the American Society of Echocardiography, Heart Rhythm Society, International Society for Adult Congenital Heart Disease, Society for Cardiovascular Angiography and Interventions, and Society of Thoracic Surgeons. J. Am. Coll. Cardiol. 52, e143–e263.
Welsman, J., Bywater, K., Farr, C., Welford, D., Armstrong, N., 2005. Reliability of peak VO(2) and maximal cardiac output assessed using thoracic bioimpedance in children. Eur. J. Appl. Physiol. 94, 228–234.
Willemsen, G.H., de Geus, E.J., Klaver, C.H., Van Doornen, L.J., Carroll, D., 1996. Ambulatory monitoring of the impedance cardiogram. Psychophysiology 33, 184–193.
Zomer, A.C., Vaartjes, I., Uiterwaal, C.S., van der Velde, E.T., van den Merkhof, L.F., Baur, L.H., Ansink, T.J., Cozijnsen, L., Pieper, P.G., Meijboom, F.J., et al., 2012. Circumstances of death in adult congenital heart disease. Int. J. Cardiol. 154, 168–172.